

Using a global aerosol model adjoint to unravel the footprint of spatially-distributed emissions on cloud droplet number and cloud albedo

V. A. Karydis,¹ S. L. Capps,² R. H. Moore,³ A. G. Russell,⁴ D. K. Henze,⁵ and A. Nenes^{1,2}

Received 30 July 2012; revised 23 October 2012; accepted 29 October 2012; published 19 December 2012.

[1] The adjoints of the GEOS-Chem Chemical Transport Model and a comprehensive cloud droplet parameterization are coupled to study the sensitivity of cloud droplet number concentration (N_d) over US regions and Central Europe to global emissions of anthropogenic fine mode aerosol precursors. Simulations reveal that the N_d over the midwestern and southeastern US is mostly sensitive to SO₂ emissions during August, and to NH₃ emissions during February. Over the western US, N_d is mostly sensitivity to SO₂ and primary organic aerosol emissions. In Central Europe, N_d is most sensitive to NH₃ and NO_x emissions. As expected, local emissions strongly affect N_d ; long-range transport, however, is also important for the western US and Europe. Emissions changes projected for the year 2050 are estimated to have the largest impacts on cloud albedo and N_d over Central Europe during August (42% and 82% change, respectively) and western US during February (12% and 36.5% change, respectively). **Citation:** Karydis, V. A., S. L. Capps, R. H. Moore, A. G. Russell, D. K. Henze, and A. Nenes (2012), Using a global aerosol model adjoint to unravel the footprint of spatially-distributed emissions on cloud droplet number and cloud albedo, *Geophys. Res. Lett.*, 39, L24804, doi:10.1029/2012GL053346.

1. Introduction

[2] Cloud droplets form upon pre-existing atmospheric aerosols, and their modulation from anthropogenic emissions has profound impacts on cloud radiative properties, the hydrological cycle and climate. The impact of aerosol on regional climate can be even stronger, owing to the variability of aerosol and regional climate sensitivity [Shindell and Faluvegi, 2010]. Attribution of climate forcing from sector-specific emissions is based on sequential perturbation calculations at the cost of a climate run per sector investigated [Shindell et al., 2009]. This approach is frequently limited by addressing only one sector (e.g., transport [Fuglestedt et al., 2008]) or by invoking approximations required to

reduce the computational burden (e.g., constant oxidant levels [Koch et al., 2007]). Adjoint modeling provides an efficient sensitivity analysis alternative to brute-force approaches and does not require perturbations in emissions. This is accomplished by propagating a differential variation of a model output (e.g., aerosol concentration) backwards through the model to express its sensitivity with respect to inputs of interest (e.g., emissions) without perturbing the model state.

[3] The GEOS-Chem chemical transport model (CTM) is a widely used global model for studying chemistry-aerosol-climate interactions [Leibensperger et al., 2012a, 2012b]. Henze et al. [2007] developed the adjoint of the code and since has been increasingly widely used, including identifying sources of black carbon deposition on the Tibetan Plateau [Kopacz et al., 2011]. Here the GEOS-Chem adjoint is coupled together with the adjoint of a comprehensive droplet parameterization [Karydis et al., 2012] to quantify the influences of global emissions of primary organic aerosol (POA) and inorganic aerosol precursors (SO₂, NO_x, and NH₃) on the predicted cloud droplet number concentration (N_d) and cloud albedo (A) within three regions of the continental US and Central Europe during August and February for 2008 and 2050.

2. Model Framework Description

[4] The GEOS-Chem model (v.9.1.1, <http://geos-chem.org>) is used to simulate the global aerosol distributions during February and August 2008, with 4° by 5° horizontal resolution and 47 pressure levels from the surface to 0.01 hPa. A detailed description of the model configuration and emissions is provided in the auxiliary material.[†] The adjoint of the GEOS-Chem model [Henze et al., 2007] computes $\frac{\partial M_{a,tot}}{\partial E_{i,j}}$, the sensitivity of total aerosol mass concentrations, over a region $M_{a,tot}$, to specific emissions E_i (where i is the emission type) for each grid cell j . In this study, $\frac{\partial M_{a,tot}}{\partial E_{i,j}}$ is calculated monthly for $M_{a,tot}$ on the final day of the month.

[5] Calculation of N_d is carried out with the Kumar et al. [2009] parameterization; droplets are formed in ascending cloud parcels that contain soluble and insoluble particles competing for water vapor. The N_d adjoint [Karydis et al., 2012] provides the sensitivity of N_d with respect to the parameterization input (updraft velocity; uptake coefficient; and hygroscopicity, adsorption, and number of each aerosol lognormal mode). The two adjoint frameworks elucidate the relationship of emissions to N_d by combining

¹Earth and Atmospheric Sciences, Georgia Institute of Technology, Atlanta, Georgia, USA.

²Chemical and Biomolecular Engineering, Georgia Institute of Technology, Atlanta, Georgia, USA.

³NASA Langley Research Center, Hampton, Virginia, USA.

⁴Civil and Environmental Engineering, Georgia Institute of Technology, Atlanta, Georgia, USA.

⁵Department of Mechanical Engineering, University of Colorado at Boulder, Boulder, Colorado, USA.

Corresponding author: A. Nenes, Earth and Atmospheric Sciences, Georgia Institute of Technology, 311 Ferst Dr., Atlanta, GA 30332-0340, USA. (athanasios.nenes@gatech.edu)

[†]Auxiliary materials are available in the HTML. doi:10.1029/2012GL053346.

the local sensitivity of N_d to aerosol number concentration, $\left. \frac{\partial N_d}{\partial N_a} \right|_r$ for cells in a specific region of interest, r , (converted into local sensitivity of N_d to aerosol mass concentration, $\left. \frac{\partial N_d}{\partial M_a} \right|_r$, following the aerosol mass to number conversion as presented by Karydis *et al.* [2011]), with the sensitivity of total aerosol mass concentrations to anthropogenic emissions from each grid cell of the model, $\frac{\partial M_{a,tot}}{\partial E_{i,j}}$, obtained from the GEOS-

Chem adjoint. The result is the “footprint” (or impacts expressed as the sensitivity) of anthropogenic emissions from each grid cell on the droplet number over a specific region $\frac{\partial N_{d,tot}}{\partial E_{i,j}} = \left(\sum_{r=1}^R \left. \frac{\partial N_d}{\partial M_a} \right|_r \right) \left(\frac{\partial M_{a,tot}}{\partial E_{i,j}} \right)$, where R is the total number of cells in the region. The relative importance of anthropogenic emissions from each grid cell are presented as fully normalized sensitivities, $R_{i,j} = \frac{E_{i,j}}{N_d} \frac{\partial N_d}{\partial E_{i,j}} = \frac{\partial \ln N_d}{\partial \ln E_{i,j}}$, N_d is

the N_d over the region of study. $R_{tot,j}$ expresses the contribution of total anthropogenic emissions from grid cell j on N_d and $R_{i,tot}$ expresses the total (worldwide) contribution of anthropogenic emissions of type i (NH_3 , SO_2 , NO_x , or POA) on N_d . A detailed description of the sensitivity calculations is provided in the auxiliary material.

[6] The sensitivity results can be used to estimate the change in future N_d and cloud albedo, especially since adjoint sensitivities tend to be more robust than traditional source-receptor relationships determined from perturbing emissions across broad spatial scales [Turner *et al.*, 2012]. We consider projected aerosol precursor emissions following the Representative Concentration Pathway 4.5 (RCP4.5; Table S2 in Text S1), where total radiative forcing is stabilized before 2100 by employment of a range of technologies and strategies for reducing greenhouse gas emissions [Clarke *et al.*, 2007]. Using the projected emissions change between 2010 and 2050, the change in N_d , ΔN_d , for each region is calculated for February and August. The first order change in cloud albedo (ΔA) is calculated from ΔN_d by integrating the susceptibility of A to N_d , $\frac{\partial A}{\partial N_d} = \frac{A(1-A)}{3N_d}$

[Twomey, 1991] over each region between 2010 and 2050 values. Cloud albedo at 2050, A_{2050} , is then given by

$$A_{2050} = \frac{C}{1+C}, \text{ where } C = \left(1 + \frac{\Delta N_d}{N_{d,2010}} \right)^{1/3} \left(\frac{A_{2010}}{1-A_{2010}} \right)$$

and A_{2010} , $N_{d,2010}$ are the local values of albedo and N_d at 2010, respectively. ΔA is then equal to $A_{2050} - A_{2010}$. Values of A_{2010} are obtained by differencing NASA CERES satellite total sky and clear sky albedos for February and August [Acker and Leptoukh, 2007] as described in Moore *et al.* [2012]. These calculations give an upper limit on albedo change since liquid water feedbacks which mitigate microphysical changes are not considered [Stevens and Feingold, 2009]. Given the lack of explicit microphysics in this study, a required assumption is that the aerosol number size distribution shape remains unchanged in the future. This may induce some error in the predicted sensitivity; as differences in aerosol microphysical processes may change the relationship between emissions and CCN concentrations.

Toward this, Manktelow *et al.* [2009] found that the aerosol number potential of N. American and Asian emissions was a factor of 3 to 4 times larger than that of European emissions, resulting in a 70% more efficient production of CCN.

3. Results and Discussion

[7] Figure 1 presents the fully normalized sensitivity of regional N_d to anthropogenic emissions from each grid cell. Figures 2 (top) and 2 (bottom) depict the total worldwide contribution of anthropogenic emissions on N_d as well as the fractional contribution of these anthropogenic emissions from within each region for present and future (based on RCP4.5 scenario) conditions, respectively. An analysis of each region and species follows.

[8] *Midwestern United States.* N_d is mostly sensitive to SO_2 ($R_{\text{SO}_2,tot} = 8.6 \times 10^{-2}$) and NO_x ($R_{\text{NO}_x,tot} = 3.4 \times 10^{-2}$) during August, and to NH_3 emissions during February ($R_{\text{NH}_3,tot} = 6.3 \times 10^{-2}$). Moreover, the high impact of NH_3 emissions on N_d during February together with the low impact of NO_x emissions, confirms that NH_3 is the limiting reactant in the formation of ammonium nitrate during the winter in this area. POA emissions have relatively low impact ($\sim 0.5 \times 10^{-2}$) on N_d , (Figure 2) owing to the lower magnitude of the primary organic emissions, compared to inorganic precursors over the midwestern US. The importance of NH_3 emissions in February and SO_2 emissions in August to aerosol formation over the midwestern US was also confirmed by Tsimpidi *et al.* [2007]. Henze *et al.* [2009] also predicted similar trends for the sensitivity of inorganic aerosols to NH_3 and SO_2 , however; the predicted effect on N_d is less pronounced as only a small fraction of aerosols is activated into droplets (<5%) over the polluted continental environments such as midwestern US. The lower impact of NO_x emissions on N_d during February is in accordance with Tsimpidi *et al.* [2008], who attributed this behavior to the increase of oxidants levels (after a NO_x emission reduction during winter) which promoted secondary aerosol production and compensated for the decrease of nitrates. In August, sulfate is the dominant inorganic aerosol component; therefore, aerosol concentrations are more sensitive to SO_2 emission changes from electricity generating units, followed by NO_x emissions, while NH_3 emissions have little impact (Figure 2). N_d is predicted to decrease by 75.62 cm^{-3} (9.87%) and 26.05 cm^{-3} (3.4%) due to SO_2 and NO_x emission changes by 2050, respectively (Table S3 in Text S1). During February, SO_2 emission decreases will increase the free NH_3 in the atmosphere, resulting in an increase in ammonium nitrate concentration. Therefore, sulfate is replaced by nitrate in the aerosol phase resulting in a minimal negative response of N_d to SO_2 emission changes ($R_{\text{SO}_2,tot} = -0.28 \times 10^{-2}$). The negative sensitivity arises from sufficiently low temperatures and high concentrations of HNO_3 at which the addition of one mole of SO_4^{-2} to the aerosol can actually reduce the total mass by displacing two moles of NO_3^- [Moya *et al.*, 2002; West *et al.*, 1999]. Overall, during August, N_d and A are predicted to decrease in 2050 by $\sim 100 \text{ cm}^{-3}$ (13.2% change from 2010 levels) and $\sim 4 \times 10^{-3}$ (4.2%), respectively (Table S3 in Text S1). During February, ΔA and ΔN_d are predicted to be very low (Table S3 in Text S1). In this case, $R_{\text{SO}_2,tot}$ and $R_{\text{NO}_x,tot}$ are very small, while $R_{\text{NH}_3,tot}$ is high (and NH_3 emissions are

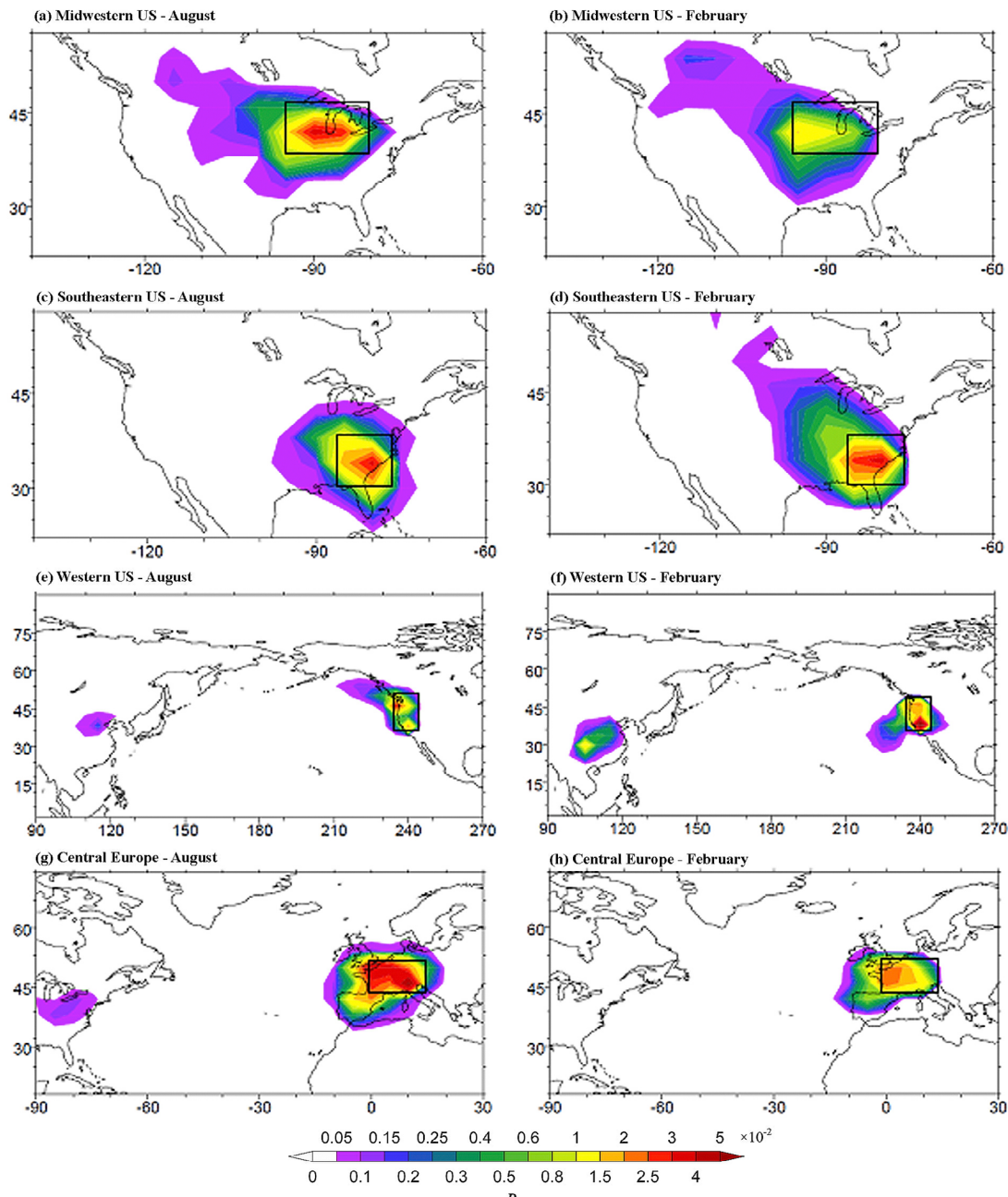


Figure 1. Contribution of total anthropogenic emissions to cloud droplet number concentration over (a, b) Midwest US, (c, d) Southeast US, (e, f) Western US, and (g, h) Central Europe during (left) August and (right) February of 2008. The regions of study are denoted by the squares.

expected to slightly increase in the future) (Figure 2, top) so emissions changes have a small impact on N_d and A .

[9] *Southeastern United States.* N_d over the southeastern US is more sensitive to SO_2 electricity generation emissions during both seasons (5.9×10^{-2}) followed by NH_3 emissions from agriculture during February (5.1×10^{-2}) and NO_x emissions from electricity generating units during August (2.8×10^{-2}) (Figure 2). Consistent with *Capps et al.* [2012], the low amounts of nitric acid and ammonia not “bound” to sulfate leads to low levels of aerosol ammonium nitrate. This means that the aerosol cannot buffer SO_2 emissions shifts. N_d is predicted to decrease by 39 cm^{-3} (5.9%) and 57 cm^{-3} (10%) due to SO_2 emission changes

by 2050 during August and February, respectively, and by 16 cm^{-3} (2.5%) due to NO_x emissions changes during August (Table S3 in Text S1). Anthropogenic POA emissions have an important impact during both February and August ($R_{\text{POA},\text{tot}} = 2.2 \times 10^{-2}$ and 1.1×10^{-2} , respectively). Nevertheless, the predicted N_d change attributed to POA emission changes by 2050 is negligible (less than 0.1%) since the latter is not expected to change significantly over US (Table S2 in Text S1). Overall, N_d and A are predicted to decrease in 2050 by $\sim 53.3 \text{ cm}^{-3}$ (8.3%) and 3.5×10^{-3} (2.5%), respectively, during August and by 56.7 cm^{-3} (10%) and 5.1×10^{-3} (2.8%), respectively, during February (Table S3 in Text S1).

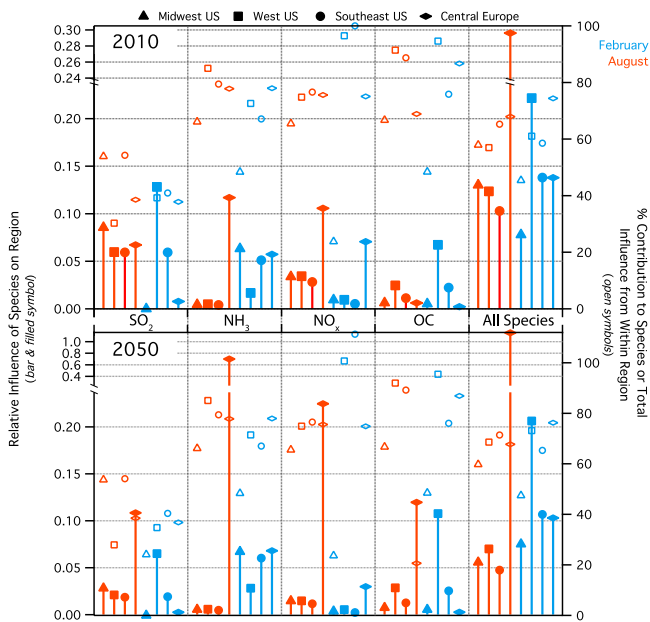


Figure 2. Total contribution of anthropogenic SO_2 , NO_x , NH_3 , and OC emissions to N_d over Midwest US, Southeast US, Western US, and Central Europe during August (orange) and February (blue) of (top) 2010 and (bottom) 2050. The fractional contribution of anthropogenic emissions from within each region on N_d is also shown (open symbols).

[10] *Western US:* Anthropogenic SO_2 emissions are found to be the most important contributor to cloud droplet formation over the western US during both February and August ($R_{\text{SO}_2, \text{tot}} = 12.8 \times 10^{-2}$ and 6×10^{-2} , respectively) (Figure 2). SO_2 emissions contribution to N_d over western US is similar (during August) or even higher (during February) than the corresponding contribution to N_d over midwestern and southeastern US, despite the fact that typically SO_2 emissions are lower in western US. This can be explained by the high sensitivity of N_d to SO_2 from long range transport, especially from eastern China, resulting in a significant decrease of N_d in 2050 (52.6 cm^{-3} or 20.5%) due to changes on SO_2 emissions outside the western US. SO_2 emissions from shipping also contribute significantly to N_d . POA anthropogenic emissions also significantly impact the N_d over the West, especially during February ($R_{\text{POA}, \text{tot}} = 6.7 \times 10^{-2}$). Similarly to southeastern US though, the predicted ΔN_d in 2050 due to POA emission changes is low (Table S3 in Text S1). Anthropogenic NH_3 emissions during August and anthropogenic NO_x emissions during February do not significantly impact N_d over the West ($R_{\text{NH}_3, \text{tot}} = 0.5 \times 10^{-2}$ and $R_{\text{NO}_x, \text{tot}} = 1 \times 10^{-2}$, respectively) (Figure 2). Although highly concentrated centers of agricultural or urban activity emit significant amounts of NO_x and NH_3 , respectively, pristine surrounding land causes dilution that limits the apparent impact on aerosol formation. Overall, N_d and A are predicted to decrease in 2050 by 52.6 cm^{-3} (12.2%) and 2.6×10^{-3} (4%), respectively, during August and by 93.5 cm^{-3} (36.5%) and 17.1×10^{-3} (12.3%), respectively, during February (Table S3 in Text S1). The strong effect of long-range transport of pollutants is mostly evident during February where the 57% of the predicted ΔN_d in 2050 is attributed to

changes on anthropogenic emissions from outside the western US.

[11] *Central Europe.* N_d is mostly sensitive to NH_3 ($R_{\text{NH}_3, \text{tot}} = 11.7 \times 10^{-2}$) and NO_x ($R_{\text{NO}_x, \text{tot}} = 10.6 \times 10^{-2}$) emissions during both August and February ($R_{\text{NH}_3, \text{tot}} = 5.7 \times 10^{-2}$ and $R_{\text{NO}_x, \text{tot}} = 7.1 \times 10^{-2}$). POA emissions impact N_d negligibly over Central Europe during both seasons ($R_{\text{POA}, \text{tot}}$ as low as 0.2×10^{-2}). These conclusions are consistent with *Megaritis et al.* [2012] who found that NH_3 emissions had the most significant impact on aerosol formation over Europe, while the impact of POA emissions was the smallest. Ammonium nitrate is a major aerosol component over Europe; therefore, emissions of its gas phase precursors (NH_3 and NO_x) exhibit the strongest impact on the inorganic aerosol population and N_d . However, according to RCP4.5 scenario, emissions of NH_3 over central Europe are not expected to change significantly by 2050 (0.06% increase). On the other hand, changes on NO_x emissions result to significant changes on ΔN_d (315 cm^{-3} or 50% and 74 cm^{-3} or 10% during August and February, respectively). SO_2 also contributes with a similar magnitude to N_d over central Europe during August ($R_{\text{SO}_2, \text{tot}} = 6.7 \times 10^{-2}$). N_d is predicted to decrease by 230 cm^{-3} (37%) due to SO_2 emission changes by 2050 and is strongly influenced by long-range transport of SO_2 from Midwestern and northeastern US. The predicted ΔN_d due to changes of anthropogenic SO_2 emissions from outside the central Europe during August is 230 cm^{-3} (23%). During February, when sulfate levels are lower, N_d is less sensitive to SO_2 emissions ($R_{\text{SO}_2, \text{tot}} = 0.8 \times 10^{-2}$), likely due to the limited H_2O_2 availability over Europe during this season [*Megaritis et al.*, 2012]. Overall, ΔN_d decrease by 510 cm^{-3} (82%) and ΔA by 31.86×10^{-3} (42%), during August. The large $R_{\text{SO}_2, \text{tot}}$ and $R_{\text{NO}_x, \text{tot}}$ predicted over Europe during this season (Figure 2), together with the large future reductions of these emissions (e.g., SO_2 ; Figure 1) results in the strong response of N_d and A to future emission changes, which is also influenced by the long-range impact of SO_2 emission reductions from the US (Figure 1). During February, ΔN_d and ΔA are predicted to be 77 cm^{-3} (10.7%) and 4.2×10^{-3} (3.2%), respectively, and are mostly attributed to NO_x emissions (Table S3 in Text S1).

4. Conclusions

[12] In this work, the adjoints of the GEOS-Chem CTM and *Kumar et al.* [2009] droplet parameterization are used to determine the source region and relative impact of aerosol precursor emissions on N_d and albedo. Assessments are carried out for specific regions in February and August of 2008 and 2050 (using the RCP4.5 scenario). Among all species, the influence of sulfate emissions in August is most similar across regions, comprising at least 50% (20%) of the total influence in the US regions (Central Europe). For each region, the percent contribution from sulfate emissions within the region is the lowest of all the species tracked, which implicates long-range transport of significant sulfate burdens. Central Europe N_d in August is far more influenced by NH_3 and NO_x emissions than any region over the US due to the large contribution of ammonium nitrate aerosol to the regional aerosol. Nevertheless, for all four regions, 65–85% of the influence from NH_3 and NO_x emissions came from within the region in August. In February, the influence of NO_x emissions on Central Europe N_d remains much higher

than on the N_d over US regions. However, the impact of NH_3 emissions on N_d , during February, is similar for Central Europe, midwestern, and southeastern US. Additionally, the maximum percent contribution of NO_x emissions within the region (nearly 100%) is attained in the western and southeastern US in February. The strongest internal influence is from POA in both August and February, owing to the shorter lifetime of the species. With the exception of the western US, the relative influence of POA on N_d is minor. The influence of different emissions mixes on N_d is most apparent from the distinction between the US and European response to NO_x and NH_3 emissions. Based on the RCP4.5 scenario and the 2008 adjoint, A in Central Europe during August and in western US during February is most strongly affected by future emission changes, owing to the effects of long-range transport of anthropogenic emissions (mainly SO_2) and NO_x reductions over Central Europe and the western US. The significant decrease of N_d over these regions results in higher anthropogenic emissions contributions to N_d in 2050 as the maximum supersaturation and droplet activation fractions are increased [Karydis et al., 2012]. In other regions and seasons, the anthropogenic emissions contributions to N_d are lower in 2050, mainly due to the significant decrease of SO_2 and NO_x emissions over the US and Europe (Figure 2, bottom). The above results reveal N_d sensitivities that would not have been predicted from earlier forward sensitivity analyses, (i.e., the importance of SO_2 long-range transport on N_d over western US or the increasing contribution of SO_2 to N_d over central Europe in the future), and can be used from policy makers to effectively design future emission control strategies.

[13] Understanding relative impacts in coupled complex models is a challenge. Using the coupled adjoint sensitivity modeling framework developed here has allowed us to quantify the sensitivity of cloud droplet formation and cloud albedo to different aerosol precursor emissions and to unravel the importance of sectoral, spatial, and seasonal emissions.

[14] **Acknowledgments.** We acknowledge support from NASA-ACMAP and NOAA. SLC gratefully acknowledges the NSF GRF and NASA ESSF. DKH acknowledges support from a NASA New Investigator grant (NNX10AR06G). We also thank two anonymous reviewers for comments that improved the manuscript.

[15] The editor thanks two anonymous reviewers for their assistance in evaluating this paper.

References

- Acker, J. G., and G. Leptoukh (2007), Online analysis enhances use of NASA Earth science data, *Eos Trans. AGU*, 88(2), 14, doi:10.1029/2007EO020003.
- Capps, S., D. Henze, A. Hakami, A. Russell, and A. Nenes (2012), ANISORROPIA: The adjoint of the aerosol thermodynamic model ISORROPIA, *Atmos. Chem. Phys.*, 12, 527–543, doi:10.5194/acp-12-527-2012.
- Clarke, L., J. Edmonds, H. Jacoby, H. Pitcher, J. Reilly, and R. Richels (2007), Scenarios of greenhouse gas emissions and atmospheric concentrations: Synthesis and Assessment Product 2.1, *Rep. 2.1A*, 154 pp., Off. of Biol. and Environ. Res., Dep. of Energy, Washington, D. C.
- Fuglestedt, J., T. Berntsen, G. Myhre, K. Rypdal, and R. B. Skeie (2008), Climate forcing from the transport sectors, *Proc. Natl. Acad. Sci. U. S. A.*, 105(2), 454–458, doi:10.1073/pnas.0702958104.
- Henze, D. K., A. Hakami, and J. H. Seinfeld (2007), Development of the adjoint of GEOS-Chem, *Atmos. Chem. Phys.*, 7(9), 2413–2433, doi:10.5194/acp-7-2413-2007.
- Henze, D. K., J. H. Seinfeld, and D. T. Shindell (2009), Inverse modeling and mapping US air quality influences of inorganic $\text{PM}_{2.5}$ precursor emissions using the adjoint of GEOS-Chem, *Atmos. Chem. Phys.*, 9(16), 5877–5903, doi:10.5194/acp-9-5877-2009.
- Karydis, V. A., P. Kumar, D. Barahona, I. N. Sokolik, and A. Nenes (2011), On the effect of dust particles on global cloud condensation nuclei and cloud droplet number, *J. Geophys. Res.*, 116, D23204, doi:10.1029/2011JD016283.
- Karydis, V. A., S. L. Capps, A. G. Russell, and A. Nenes (2012), Adjoint sensitivity of global cloud droplet number to aerosol and dynamical parameters, *Atmos. Chem. Phys.*, 12(9), 9041–9055, doi:10.5194/acp-12-9041-2012.
- Koch, D., T. C. Bond, D. Streets, and N. Unger (2007), Linking future aerosol radiative forcing to shifts in source activities, *Geophys. Res. Lett.*, 34, L05821, doi:10.1029/2006GL028360.
- Kopacz, M., D. L. Mauzerall, J. Wang, E. M. Leibensperger, D. K. Henze, and K. Singh (2011), Origin and radiative forcing of black carbon transported to the Himalayas and Tibetan Plateau, *Atmos. Chem. Phys.*, 11, 2837–2852.
- Kumar, P., I. N. Sokolik, and A. Nenes (2009), Parameterization of cloud droplet formation for global and regional models: Including adsorption activation from insoluble CCN, *Atmos. Chem. Phys.*, 9(7), 2517–2532, doi:10.5194/acp-9-2517-2009.
- Leibensperger, E. M., L. J. Mickley, D. J. Jacob, W. T. Chen, J. H. Seinfeld, A. Nenes, P. J. Adams, D. G. Streets, N. Kumar, and D. Rind (2012a), Climatic effects of 1950–2050 changes in US anthropogenic aerosols—Part 1: Aerosol trends and radiative forcing, *Atmos. Chem. Phys.*, 12(7), 3333–3348, doi:10.5194/acp-12-3333-2012.
- Leibensperger, E. M., L. J. Mickley, D. J. Jacob, W. T. Chen, J. H. Seinfeld, A. Nenes, P. J. Adams, D. G. Streets, N. Kumar, and D. Rind (2012b), Climatic effects of 1950–2050 changes in US anthropogenic aerosols—Part 2: Climate response, *Atmos. Chem. Phys.*, 12(7), 3349–3362, doi:10.5194/acp-12-3349-2012.
- Manktelow, P. T., K. S. Carslaw, G. W. Mann, and D. V. Spracklen (2009), Variable CCN formation potential of regional sulfur emissions, *Atmos. Chem. Phys.*, 9(10), 3253–3259, doi:10.5194/acp-9-3253-2009.
- Megaritis, A. G., C. Fountoukis, P. E. Charalampidis, C. Pilinis, and S. N. Pandis (2012), Response of fine particulate matter concentrations to changes of emissions and temperature in Europe, *Atmos. Chem. Phys. Discuss.*, 12(4), 8771–8822, doi:10.5194/acpd-12-8771-2012.
- Moore, R. H., V. A. Karydis, S. L. Capps, T. L. Latham, and A. Nenes (2012), Droplet number prediction uncertainties from CCN: An integrated assessment using observations and a global adjoint model, *Atmos. Chem. Phys. Discuss.*, 12, 20,483–20,517, doi:10.5194/acpd-12-20483-2012.
- Moya, M., S. N. Pandis, and M. Z. Jacobson (2002), Is the size distribution of urban aerosols determined by thermodynamic equilibrium? An application to Southern California, *Atmos. Environ.*, 36(14), 2349–2365, doi:10.1016/S1352-2310(01)00549-0.
- Shindell, D., and G. Faluvegi (2010), The net climate impact of coal-fired power plant emissions, *Atmos. Chem. Phys.*, 10, 3247–3260, doi:10.5194/acp-10-3247-2010.
- Shindell, D. T., G. Faluvegi, D. M. Koch, G. A. Schmidt, N. Unger, and S. E. Bauer (2009), Improved attribution of climate forcing to emissions, *Science*, 326(5953), 716–718, doi:10.1126/science.1174760.
- Stevens, B., and G. Feingold (2009), Untangling aerosol effects on clouds and precipitation in a buffered system, *Nature*, 461(7264), 607–613, doi:10.1038/nature08281.
- Tsimpidi, A. P., V. A. Karydis, and S. N. Pandis (2007), Response of inorganic fine particulate matter to emission changes of sulfur dioxide and ammonia: The eastern United States as a case study, *J. Air Waste Manage. Assoc.*, 57(12), 1489–1498, doi:10.3155/1047-3289.57.12.1489.
- Tsimpidi, A. P., V. A. Karydis, and S. N. Pandis (2008), Response of fine particulate matter to emission changes of oxides of nitrogen and anthropogenic volatile organic compounds in the eastern United States, *J. Air Waste Manage. Assoc.*, 58(11), 1463–1473, doi:10.3155/1047-3289.58.11.1463.
- Turner, A. J., D. K. Henze, R. V. Martin, and A. Hakami (2012), The spatial extent of source influences on modeled column concentrations of short-lived species, *Geophys. Res. Lett.*, 39(12), L12806, doi:10.1029/2012GL051832.
- Twomey, S. (1991), Aerosols, clouds and radiation, *Atmos. Environ., Part A*, 25(11), 2435–2442, doi:10.1016/0960-1686(91)90159-5.
- West, J. J., A. S. Ansari, and S. N. Pandis (1999), Marginal $\text{PM}_{2.5}$: Nonlinear aerosol mass response to sulfate reductions in the eastern United States, *J. Air Waste Manage. Assoc.*, 49(12), 1415–1424, doi:10.1080/10473289.1999.10463973.